

This article was downloaded by:

On: 30 January 2011

Access details: *Access Details: Free Access*

Publisher *Taylor & Francis*

Informa Ltd Registered in England and Wales Registered Number: 1072954 Registered office: Mortimer House, 37-41 Mortimer Street, London W1T 3JH, UK



## Separation & Purification Reviews

Publication details, including instructions for authors and subscription information:

<http://www.informaworld.com/smpp/title~content=t713597294>

### Molecular Separation Barriers and Their Application to Catalytic Reactor Design

C. R. Robertson<sup>a</sup>; A. S. Michaels<sup>b</sup>; L. R. Waterland<sup>c</sup>

<sup>a</sup> Department of Chemical Engineering, Stanford University Stanford, CA <sup>b</sup> ALZA Corporation, Palo Alto, CA <sup>c</sup> Acurex Corporation, Mountain View, CA

**To cite this Article** Robertson, C. R. , Michaels, A. S. and Waterland, L. R.(1976) 'Molecular Separation Barriers and Their Application to Catalytic Reactor Design', *Separation & Purification Reviews*, 5: 2, 301 — 332

**To link to this Article: DOI:** 10.1080/03602547608069358

**URL:** <http://dx.doi.org/10.1080/03602547608069358>

### PLEASE SCROLL DOWN FOR ARTICLE

Full terms and conditions of use: <http://www.informaworld.com/terms-and-conditions-of-access.pdf>

This article may be used for research, teaching and private study purposes. Any substantial or systematic reproduction, re-distribution, re-selling, loan or sub-licensing, systematic supply or distribution in any form to anyone is expressly forbidden.

The publisher does not give any warranty express or implied or make any representation that the contents will be complete or accurate or up to date. The accuracy of any instructions, formulae and drug doses should be independently verified with primary sources. The publisher shall not be liable for any loss, actions, claims, proceedings, demand or costs or damages whatsoever or howsoever caused arising directly or indirectly in connection with or arising out of the use of this material.

MOLECULAR SEPARATION BARRIERS AND THEIR APPLICATION  
TO CATALYTIC REACTOR DESIGN

C.R. Robertson  
Department of Chemical Engineering  
Stanford University  
Stanford, CA 94305

A.S. Michaels  
ALZA Corporation  
Palo Alto, CA 94304

L.R. Waterland  
Acurex Corporation  
Mountain View, CA 94042

ABSTRACT

The use of semipermeable membranes for multicomponent separations based on molecular size has long been recognized. In certain applications, however, it is often desirable not to effect a separation of chemical constituents, but to sustain a separation which already exists. As an example, the efficient and economical design of a chemical reactor using an enzyme as a catalyst depends on the accessibility of the reactant to the catalyst as well as on the degree to which a physical separation between the enzyme and the reactor product stream is maintained. A particularly simple and attractive means of achieving this is through the use of semipermeable asymmetric hollow fiber membranes. For example, by

sequestering an enzyme solution within the annular macroporous support regions of an asymmetric hollow fiber, a physical separation between enzyme and a reactant solution flowing through the fiber lumen is achieved. In this way, small reactant molecules are free to diffuse across the ultrathin membrane skin into the open-cell support structure where reaction will occur. Product molecules will diffuse back into the lumen, and a compact chemical reactor results. The operating behavior of this type of catalytic reactor will be described and its application to the hydrolysis of  $\alpha$ -nitro-phenyl- $\beta$ -D-galactopyranoside and of lactose is discussed.

#### INTRODUCTION

Enzymes are protein molecules which catalyze the chemical reactions occurring in living systems. As catalysts, enzymes are characterized by high turnover numbers at room temperature and atmospheric pressure, and high specificity in that each enzyme catalyzes a single reaction or at most a closely related group of reactions. As such, enzymes have become of great industrial interest, especially in the food and pharmaceutical industries.

The economic and efficient use of enzymes as industrial catalysts has awaited the development of a suitable means whereby these relatively expensive proteins are made easily accessible to the reactant stream while at the same time kept physically separated from the reaction products. To this end, numerous techniques for enzyme immobilization by chemical coupling to, or physical entrapment within solid phases have been described and tested.<sup>1-5</sup> An undesirable characteristic common to these techniques is almost invariably a reduction in enzyme activity consequent to the immobilization process. This usually is caused either by partial denaturation of the enzyme following its immobilization or interference with enzyme/substrate interaction due to steric hindrance. Furthermore, the apparent enzyme activity may be reduced due to elution and loss of the enzyme from the support, or

to diffusional limitations on the access of substrate to or removal of product from the enzyme active sites.

In part to overcome some of these drawbacks, other immobilization techniques have focused on the notion of separating an enzyme solution from the reactant/product stream by a membrane having permeability characteristics which retain the protein but permit the passage of small substrate and product components. The primary advantage here, is the elimination of steric hindrance and possible enzyme deactivation due to binding at or near the active site since the enzyme remains free in solution and is otherwise not chemically altered. Examples of this approach include the use of semipermeable microcapsules by Chang, et al.<sup>6</sup> to contain an enzyme solution within a spherical nylon capsule formed at the boundary between two liquid phases, and the proposal by Rony<sup>7,8</sup> that cylindrical microcapsules be fabricated by filling the lumen of membrane hollow fibers and sealing the two ends. However, even these membrane-based techniques have their limitations. Chang's microencapsulation procedure is limited by substantial enzyme denaturation encountered during the interfacial polymerization step essential to microcapsule formation; whereas Rony's enzyme containing fibers method would require unrealistic control of substrate fluid flow within a fiber bundle to achieve uniform flow distribution thereby ensuring minimal fluid stagnation and consequent diffusional resistances to mass transfer.

The goal of the work described herein was to develop, characterize, and demonstrate the feasibility of an alternate approach to enzyme immobilization using asymmetric hollow fibers which would reduce or eliminate the disadvantages experienced with other schemes while at the same time offering several advantages inherent to membrane separation systems. A few of the advantages envisioned were a) an enormous surface area to reactor volume ratio, b) a hydrodynamically low shear environment for the enzyme solution, c) protection of the enzyme from macromolecular contaminants in the feed stream such as proteolytic enzymes, and d) extreme ease

of enzyme regeneration or replacement. In addition, the simplicity of the hollow fiber geometry would permit development of a mathematical description of the behavior of a hollow fiber reactor without relying on empirically adjustable parameters. Such a model would provide a very potent design tool, this being an important element not readily associated with other immobilization techniques.

The first section of this review describes the asymmetric hollow fiber immobilization technique and discusses a mathematical model developed to predict hollow fiber reactor performance. Next, experiments with a "model" enzyme-substrate system employed to confirm the theoretical predictions and to demonstrate feasibility of the technique are described. Finally, some preliminary experiments using an enzyme available in commercial quantities for lactose hydrolysis are considered.

CATALYTIC REACTOR DESIGN USING ASYMMETRIC  
HOLLOW FIBER MEMBRANES

Procedure for Enzyme Encapsulation

The availability of recently developed non-cellulosic asymmetric microporous hollow fibers suggests a new approach to enzyme immobilization using membrane separation which retains the advantages inherent in membrane encapsulation while offsetting the disadvantages. As shown by the scanning electron micrograph in Figure 1, asymmetric hollow fiber membranes are anisotropic structures, typically 350 to 900 $\mu$ m o.d. and 200 to 500 $\mu$ m i.d. consisting of a 0.1 to 0.5 $\mu$ m thick cylindrical membrane (10 to 200 $\text{\AA}$  pore size) surrounded by a 75 to 200 $\mu$ m thick annular "sponge" (5 to 10 $\mu$ m pore size). This open-cell macroporous structure is 80 to 90% void, is characterized by a large hydraulic permeability, and serves as a mechanical support for the ultrathin membrane skin. Membranes of this type are commercially available from the Amicon Corporation, Lexington, MA and from Romicon, Inc., Woburn, MA, and have a wide variety of sizes and hydraulic permeabilities. Rather than placing enzyme solution within the fiber lumen, it is possible

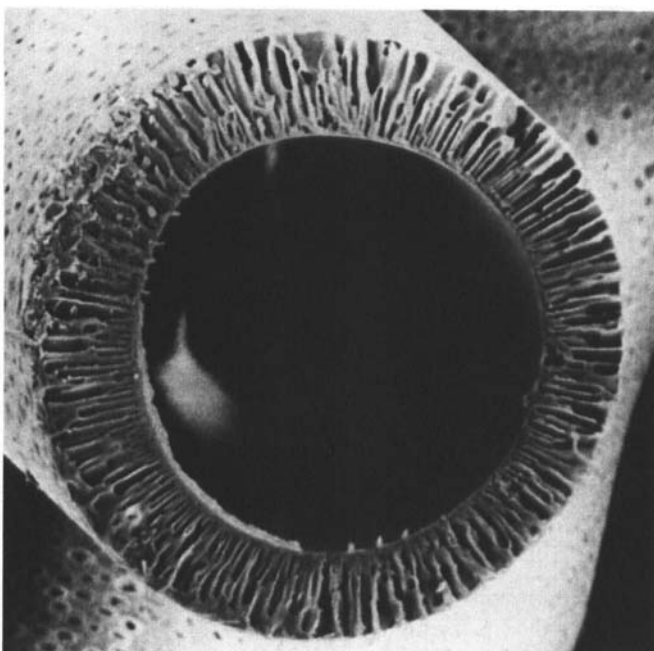


FIGURE 1

Scanning electronmicrograph of the cross-section of an asymmetric hollow fiber, magnification 300X (Photograph courtesy of Amicon Corporation, Lexington, MA) (Reproduced with permission).<sup>13</sup>

using asymmetric hollow fibers to entrain enzyme solution within the pores of the annular sponge region of a fiber and pass substrate solution through the fiber lumen. So long as the pores in the skin are too small to pass enzyme molecules, but adequately large freely to pass substrate and product, enzyme confined in the annular space external to the skin layer can act upon substrate molecules delivered by diffusion from solution flowing in the lumen without migration and loss of enzyme. Under these conditions, as shown in Figure 2, the enzyme is indeed "immobilized" or sequestered since, owing to its size, it cannot pass through the matrix of the ultra-thin skin. On the other hand, it is prevented from

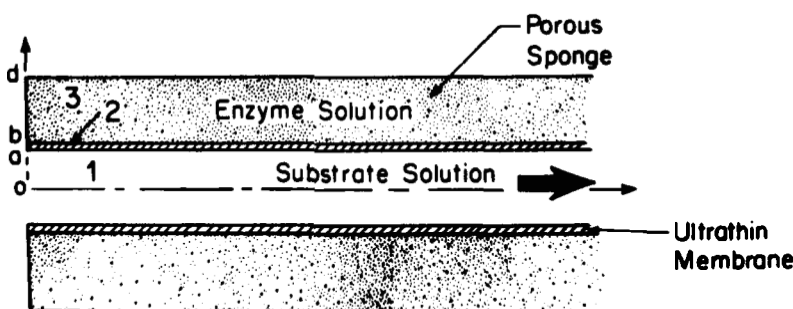
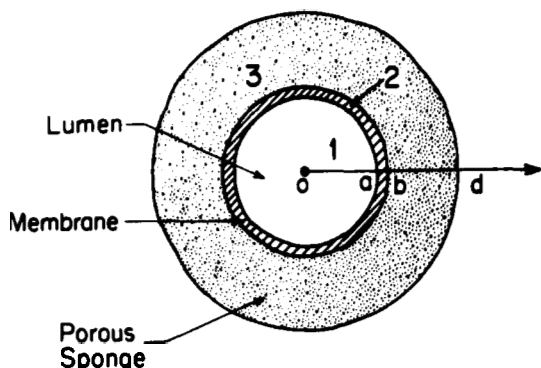


FIGURE 2

Schematic of an asymmetric hollow fiber (Reproduced with permission).<sup>10</sup>

leaving the sponge matrix due to the sponge-gas interface at the shell-side fiber boundary. This configuration serves to minimize mass transfer diffusional resistances, thereby making it a very attractive method for enzyme immobilization since, in particular, the substrate and enzyme solutions are physically separated by only  $0.5\mu\text{m}$ .

Another very important practical advantage of this type of "immobilized" enzymatic reactor configuration is the fact that the enzyme is, in reality, only immobilized with respect to the solution flowing in the fiber lumen. By the simple expedient of flushing solution through the annular sponge, it would be possible to remove and replace the enzyme (or introduce another enzyme) as desired, without dismantling or otherwise disturbing the system. Moreover, this configuration is well suited for the conduct of multienzyme conversions, and to the use of highly labile enzymes which cannot tolerate chemical immobilization procedures.

The extrapolation of this approach to a multi-fiber reactor is obvious. Hollow fiber tube modules containing 1,000 - 12,000 asymmetric fibers potted in epoxy or silicone and mounted in a lucite case are readily available,<sup>9</sup> and large-scale systems embodying multiple module assemblies are now under development. By saturating the sponge matrix of each fiber with enzyme solution and flowing substrate through each fiber lumen, a compact enzyme reactor results.

#### Theoretical Design Considerations

With the enzyme sequestered within the macroporous support region of an asymmetric hollow fiber as just described, it is possible to account exactly for the membrane-and hydrodynamic diffusional resistances to substrate-and product mass transfer. To investigate the manner in which various kinetic and diffusion parameters influence the behavior of a multitube reactor utilizing this type of enzyme placement, a theoretical analysis was developed to simulate the reactor operation under a variety of conditions. The details of this mathematical analysis are available elsewhere;<sup>10</sup> hence only the major assumptions used in constructing the model will be presented herein. Applications of the model will be demonstrated in a later section dealing with the experimental aspects of this investigation.

Mathematical Development

The idealized asymmetric hollow fiber used in the theoretical analysis is shown in Figure 2. It consists of a cylindrical tube divided into three regions: region 3 is the porous sponge section of the fiber wall, region 2 is the dense ultrathin membrane, and region 1 is the tube lumen. Laminar flow of substrate (and product) is assumed in region 1 with substrate (and product) diffusing throughout each of the three regions. Chemical reaction is confined to region 3, which contains the enzyme solution. This development further assumes steady state conditions and constant fluid properties. Axial diffusion is neglected in all regions, and region 3 is assumed to contain stagnant fluid. The rate of the enzyme reaction in region 3 is described by Michaelis-Menten kinetics.

Theoretical Results

As shown previously by Waterland et al.,<sup>10</sup> the degree to which reactant is converted to product within an asymmetric hollow fiber membrane reactor of the kind described above is dependent on seven dimensionless parameters (see Nomenclature section):  $\lambda^2$ ,  $z$ ,  $\theta$ ,  $b/a$ ,  $d/a$ ,  $\theta_1/\theta_3$ ,  $\theta_1/\gamma\theta_2$ . Once these seven parameters are specified, it is possible to use the mathematical model to predict the bulk outlet product-concentration of the catalytic reactor. Moreover, it is important to recognize that selecting these parameters for an actual system is a simple task, and allows prior determination of the reactor size and operating conditions required to achieve a given reactant conversion. The manner in which this is done is outlined in the section which follows.

EXPERIMENTAL RESULTS USING ASYMMETRIC HOLLOW  
FIBER CATALYTIC REACTORSHollow-Fiber-Immobilized  $\beta$ -GalactosidaseMaterials

Asymmetric hollow fiber membranes (type XM50) were obtained from the Amicon Corporation, Lexington, MA, in the form of a 1000

fiber bundle manifolded at each end in silicone and sheathed in a cylindrical lucite case. The configuration closely resembles a typical shell and tube heat exchanger. Manufacturer's specifications state that an individual fiber is 200 $\mu$ m i.d. with a 0.5 $\mu$ m thick membrane skin and a 75 $\mu$ m thick macroporous support region. Microscopic observation confirmed this to be the case.  $\beta$ -galactosidase from *Escherichia Coli* (purified dry powder, Worthington Biochemical, Freehold, N.J.) and o-nitrophenyl- $\beta$ -d-galactopyranoside (ONPG, Sigma Chemical, St. Louis, MO) were selected as the enzyme-substrate system for the experiments. This reaction has little industrial significance, but is convenient to use since the hydrolysis product, o-nitrophenol (ONP) is easily assayed spectrophotometrically at 405 nm. This enzyme is of sufficiently high molecular weight (520,000, 4 subunits)<sup>11,12</sup> that leakage through the ultrathin skin of an XM50 fiber (nominal molecular weight cut-off of 50,000) was expected to be negligible. Subsequent experimental results showed this to be the case.

#### Enzyme Immobilization

As described previously, the immobilization technique consists of physically entraining an aqueous solution of the enzyme within the pores of the fiber annuli of a bundle of asymmetric hollow fibers. Entrapment is achieved by soaking the shell-side of the fibers with an enzyme solution. Following this, the excess enzyme solution exterior to the fibers is drained from the shell compartment. Substrate solution is then passed through each fiber lumen, yielding a continuous-flow, tubular enzyme reactor. Since the enzyme molecules are too large to pass through the ultrathin membrane, and since solution on the shell-side of the fiber bundle has been removed, the enzyme is sequestered within the macroporous sponge region and is consequently "immobilized."

All solutions were prepared in 0.1 M phosphate buffer, 1.0 mM MgCl<sub>2</sub>, 0.5 mM disodium EDTA at pH 7.24 $\pm$ 0.03. Before each experiment, the fiber bundle was cleaned of previous enzyme solution by soaking for 3 hrs in 8 M urea, followed by ultrafiltering 2 liters

of phosphate buffer through the fibers to remove the urea and denatured enzyme. The shell was then filled with 25 ml of enzyme solution of specified concentration, refrigerated at 3°C overnight, drained and refilled with 25 ml of enzyme solution of the same concentration, and gently agitated at room temperature for 3 hrs. Following this, the shell was drained, and the unit installed in the apparatus.

#### Reactor Experiments

In each experiment, substrate solution was pumped by a variable speed roller pump from a thermostated reservoir through a flowmeter into the reactor bundle. The reactor effluent passed directly through a flow cell in a UV-visible spectrophotometer (Beckman, ACTA II) permitting continuous measurement of the outlet ONP concentration. The flowmeter and the reactor were maintained at the substrate reservoir temperature. Thermistor probes inserted in the reactor inlet and outlet allowed continuous monitoring of reactor temperature. All experiments were conducted with the same hollow fiber bundle to insure consistency. The experimental apparatus is shown schematically in Figure 3.

For each experiment, the concentration of the substrate solution was prepared so that  $\Theta = 1.0$ . Before the start of an experiment, approximately one liter of buffer was passed through the reactor. Substrate flow was then begun and outlet product concentration monitored until steady state was reached. Steady state was defined to be no measurable change in outlet product concentration for a period of at least 15 min. Three substrate flow rates were chosen and used repeatedly for each bundle enzyme concentration. All experiments reported herein were made at a reactor temperature of  $26.2 \pm 0.5^\circ\text{C}$ , with the reactor inlet and outlet temperatures for a single run differing by no more than  $0.3^\circ\text{C}$ .

#### Enzyme Kinetic Constants

Prior to each experiment, the enzyme solution used to saturate the fibers was diluted to 0.03 mg/ml and assayed. As detailed

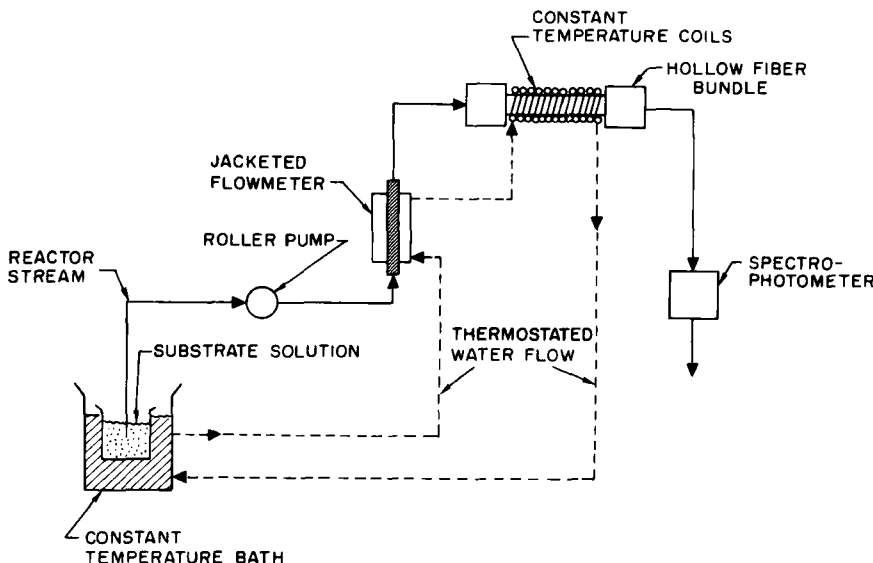


FIGURE 3

Asymmetric hollow fiber enzyme reactor apparatus (Reproduced with permission).<sup>13</sup>

by Waterland et al.,<sup>13</sup> the kinetic constants  $K_m$  and  $V_{max}$  were determined from a double reciprocal plot of initial reaction rate versus substrate concentration. Owing to dilution effects within the fiber bundle, the "fiber"  $V_{max}/K_m$  was found shown to be 84% of the "assayed"  $V_{max}/K_m$ .<sup>13</sup>

#### Substrate Diffusivity

Since the solution diffusivity of ONPG was required to compare the experimental results with the theoretical predictions, a fritted glass disk diffusion cell was used to make this measurement.<sup>13</sup> The solution diffusivity,  $D_1$ , of ONPG was measured to be  $5.4 \pm 0.4 \times 10^{-6}$  cm<sup>2</sup>/s for concentrations less than  $10^{-4}$  M.

Results

As discussed previously, the theoretical model for a simple Michaelis-Menten reaction rate predicts that reactor conversion depends on seven parameters,  $\lambda^2$ ,  $z$ ,  $\theta$ ,  $b/a$ ,  $d/a$ ,  $\delta_1/\delta_3$ , and  $\delta_1/\gamma\delta_2$ . Of these, five are fixed either by the system geometry or the choice of substrate and initial substrate concentration; hence, for these experiments

$$\theta = 1.0$$

$$\frac{b}{a} = 1.005$$

$$\frac{d}{a} = 1.75$$

$$\delta_1/\delta_3 = 1.0$$

$$\delta_1/\gamma\delta_2 = 10.0$$

The values selected for the diffusivity ratios are discussed in detail elsewhere.<sup>10</sup> Consequently, the reactor conversion is determined by the remaining two parameters

$$\lambda^2 = \frac{V_{max} a^2}{K_m \delta_3} \quad (1)$$

$$z = \frac{L \delta_1}{v_o a^2} = \frac{500 \pi L \delta_1}{Q} , \text{ for 1000 fibers} \quad (2)$$

To facilitate a direct comparison of the experimental results with the theoretical model, three values of  $z$  corresponding to three average flow rates (13.5, 35.0, and 65.2 ml/min) together with the measured active fiber length,  $L = 16.5 \pm 0.3$  cm. were used. Figure 4,

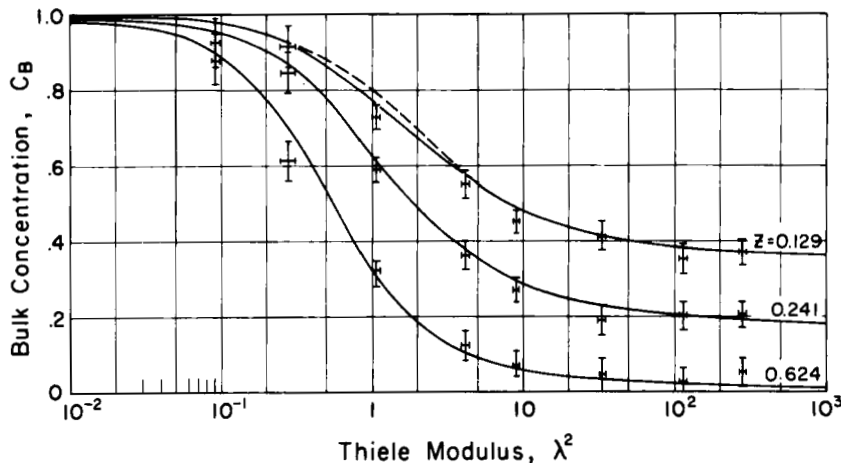


FIGURE 4

Comparison between experimental and predicted bulk substrate concentrations as a function of Thiele modulus for three dimensionless reactor lengths,  $\theta = 1.0$ . Solid lines are model predictions. See text for explanation of dashed line (Reproduced with permission).<sup>13</sup>

is a plot of the bulk outlet substrate concentration,  $C_B$ , vs  $\log \lambda^2$ . Here, the solid lines correspond to model predictions for each of the three dimensionless lengths,  $z$ . The agreement between theory and experiment is quite good.

#### Enzyme Adsorption

As mentioned earlier, the preparation of a fiber bundle included soaking in 8M urea. This step was incorporated into the preparatory procedure to insure complete denaturation of any previously entrapped enzyme, as early experimentation confirmed that ultrafiltration with water or neutral buffer was not sufficient totally to elute enzyme from the "sponge" region. Ultrafiltration of 0.1 N HCl, however, eluted the enzyme in a totally inactive form. These observations suggested that some  $\beta$ -galactosidase must be adsorbing at the fiber/solution interface.

To demonstrate conclusively that  $\beta$ -galactosidase did indeed adsorb to the fibers, an enzyme mass-balance experiment was performed.<sup>13</sup> This experiment indicated that some 10-15% of the amount of enzyme actually loaded is adsorbed; nonetheless, agreement between experimental results and theoretical model predictions (see Figure 4) which ignore enzyme adsorption is very good. This is so because, since for the degree of enzyme absorption found to occur, the extent to which the fiber bundle activity was altered was well within the overall experimental error of the kinetic measurements used to determine "fiber"  $V_{max}/K_m$ . The effects of 10-15% enzyme adsorption upon reactor conversion kinetics are too small to be detectable.

#### Enzyme Stability

$\beta$ -galactosidase immobilized by this technique was found to retain 100% activity for 60 hours of continuous reactor operation, and for 140 days when stored at 3°C.<sup>13</sup>

#### Axial Enzyme Transport

In the preceding discussion and analysis, an asymmetric hollow fiber unit has been assumed to consist of an ultrathin enzyme-impermeable membrane surrounded by an annular shell of stagnant enzyme solution. Fluid movement was considered to be confined to axial laminar flow of reactant and product within the fiber lumen. This need not always be the case, however, since the ultrathin skin and porous sponge regions possess finite hydraulic permeabilities. In particular, if the shell-side pressure were maintained below the tube-side pressure throughout the reactor, radial ultrafiltration would take place, convectively displacing enzyme from the annular sponge, and thereby removing enzyme from the reactor. However, even if net ultrafiltration was eliminated, local radial fluid flow would exist since the shell-side of the reactor is under constant hydrostatic pressure, whereas an axial pressure gradient must be maintained on the tube-side to cause axial flow of substrate solution. Thus the shell-side-to-lumen pressure difference will vanish

only at one point along the fiber. In the absence of concentration polarization and any significant osmotic pressure difference, this point would correspond to the midline of a fiber. Upstream of this point, where the lumen pressure everywhere exceeds the shell-side pressure, fluid moves radially outward, while the opposite condition applies downstream of this point. This phenomenon will have the effect of establishing a toroidal flow of ultrafiltrate exterior to the fiber lumen, which will serve to transport enzyme longitudinally from the upstream to the downstream end of a fiber. In time, therefore, the upstream portion of the bundle should become relatively depleted in enzyme, while the downstream part becomes enriched.

To assess the magnitude of this anticipated axial enzyme transport,  $\beta$ -galactosidase was labeled with the fluorescent dye fluorescein isothiocyanate.<sup>13</sup> Approximately forty fluorescent labels, on average, were attached to each enzyme molecule. This was sufficient to cause each fiber in the bundle to appear green to the unaided eye under long-wave ultraviolet illumination after soaking with a 1 mg/ml solution of labeled enzyme. This bundle was installed in the usual manner and operated with phosphate buffer at 66 ml/min, a flow rate corresponding to the largest axial pressure drop encountered in the reactor conversion experiments reported earlier. Shell, tube inlet, and tube outlet pressures were monitored. Following 100 min of operation, the bundle was removed, the lucite sheath disassembled and the exposed fibers were sectioned into ten equal lengths. Each section was incubated in 4 ml of phosphate buffer for one hour and the equilibrated fluid was assayed spectrophotometrically at 493 nm (fluorescein adsorption maximum). The axial enzyme concentration profile obtained by either method was identical and is shown in Figure 5. Indeed, a significant axial gradient in enzyme concentration was established under these operating conditions; the enzyme concentration at the downstream end of the bundle was twenty times that at the upstream end.

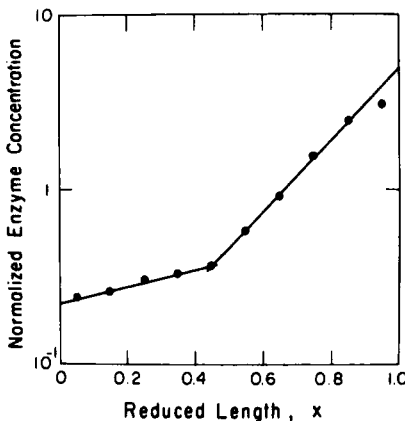


FIGURE 5

Axial enzyme concentration profile in the porous annulus after reactor operation at 66 ml/min (Reproduced with permission).<sup>13</sup>

The overall axial pressure drop along the fiber bundle was measured to be 35.5 mm Hg, in excellent agreement with a calculated axial pressure drop of 34.6 mmHg assuming Poiseuille flow and neglecting radial flow effects. The shell-side pressure equaled lumen pressure (assuming a linear axial pressure profile) at  $x = 0.42$ , rather than at  $x = 0.50$ .

This lack of radial pressure gradient symmetry about the mid-point of the bundle is most readily explained by the small but finite osmotic pressure exerted by the enzyme, which serves to increase radial outflow of fluid from the lumen in regions where lumen pressure is below shell-side pressure. Since net radial flow is zero, a larger fraction of the total fiber area must participate in inflow rather than outflow, hence the plane of no-net-radial flow must lie upstream of the midplane. There is also a change in the slope of the axial enzyme concentration profile at the point corresponding to tube-side/shell-side pressure equality (see Figure 5).

Although the exact details of the manner in which this profile is established remain unclear, the most important consideration concerns itself with the applicability of the previously developed mathematical model to a system in which the axial "sponge" enzyme concentration is not uniform as had been assumed, but instead is exponential. To examine this, the enzyme/concentration profile shown in Figure 5 was introduced into the model in a differential manner. Assuming that the profile in Figure 5 is accurate for all levels of absolute enzyme concentration, modified reactor conversions were calculated for the entire  $z = 0.129$  curve in Figure 4. The modified profile so obtained is shown as a dashed line; the consequence of axial enzyme redistribution is a slight reduction in reactor conversion efficiency. This demonstrates that even an exponential axial enzyme concentration profile does little to alter the predicted reactor conversions from those calculated assuming a uniform enzyme distribution. In fact, the only noticeable difference occurs in the region of reactor operation intermediate between kinetic control ( $\lambda^2$  small) and diffusion control ( $\lambda^2$  large). This is so because in the region of kinetic control, reactor conversion is governed solely by the total number of enzyme molecules available for reaction. Therefore, as long as the enzyme concentration gradient is sufficiently small that the entire reactor length is kinetically controlled, total reactor conversion will depend only on the total mass of enzyme in the reactor, and not its distribution. On the other hand, in the regime of strictly diffusion-control, reactor conversion is independent of enzyme concentration, hence  $\lambda^2$ . Therefore, again, as long as the enzyme axial concentration gradient is sufficiently small so that the entire reactor is diffusion controlled reactor conversion is independent of  $\lambda^2$ , hence independent of the enzyme concentration distribution.

Of course, these conclusions hold strictly only for the  $\beta$ -galactosidase system under experimental conditions used in this study, but there is reason to believe that the mathematical reactor

model which gives accurate predictions for this case will be equally applicable for other enzyme-substrate systems.  $\beta$ -galactosidase is a relatively large enzyme molecule; most other enzymes of commercial interest have much lower molecular weights, and higher diffusivities. Enzymes with higher diffusivities than  $\beta$ -galactosidase will distribute with less steep concentration profiles, and the deviations of reactor performance from that predicted by the model will be even smaller than observed here.

#### Discussion

For the  $\beta$ -galactosidase/ONPG system, an entrained-enzyme, asymmetric hollow fiber ultrafiltration membrane reactor has been shown to function as a reliable, efficient enzymatic converter. Loss of enzyme activity with time is certainly no greater, and may be less, than that of free enzyme in solution under comparable conditions. Substrate conversion efficiency correlates well with theoretical predictions.

Radial ultrafiltration under conditions of no net trans-membrane flow establishes a significant (ca. 20 fold) axial gradient of enzyme concentration along the fiber bundle. Despite this gradient, reactor performance is virtually identical to that predicted for uniform enzyme distribution except in the regime of reactor operation intermediate to diffusion control and enzyme kinetic control. In this regime, conversions are at most 4% below the predicted values.

#### Hollow-Fiber-Immobilized Lactase

Despite the extensive research efforts aimed at immobilized enzymes as well as the widespread claims of their potential impact, there are very few instances where an immobilized enzyme has been incorporated into an industrial process.<sup>14,15</sup>

One application for which recent interest has arisen, where an immobilized enzyme may find use in the near future, is the hydrolysis of lactose in milk and milk byproducts, particularly

acid whey. The utilization of acid whey, the byproduct of cottage cheese manufacture, has become of increasing concern to the dairy industry. Presently, many dairies deproteinate whey to recover valuable milk protein, but the waste stream (an acid solution, pH 4 to 6) containing about 5% lactose by weight together with lactate and various metal salts (chiefly the phosphates, sulfates and chlorides of sodium, potassium, magnesium, calcium, and iron) is of limited usefulness.<sup>16</sup> Inversion of the lactose to glucose and galactose, however, would yield a solution which could find use as a commercial sweetener.

Hence, the enzymatic hydrolysis of lactose is currently being examined in several laboratories as an alternative to the standard acid hydrolysis procedure which, to date, is economically unattractive. Commercial lactase preparations from yeast (Saccharomyces lactis) and fungal (Aspergillus niger) sources have been immobilized on porous glass<sup>17</sup>, zirconia coated porous glass<sup>18</sup>, titania<sup>19</sup>, stainless steel<sup>20</sup>, and phenol-formaldehyde resin<sup>21</sup>, and, in the case of the fungal lactase derivatives, successfully used to hydrolyze lactose in buffered lactose solutions and acid whey. The chief obstacle to industrial implementation of these schemes, however, has been the uncertain process economics associated with the support material, the enzyme, the immobilization process, and reactor regeneration following loss of enzyme activity.

Examining lactose hydrolysis seemed the logical next step toward demonstrating the viability of asymmetric hollow fiber immobilization for industrial applications, as this technique appeared particularly well suited to the lactase-lactose reaction. The substrate is of low molecular weight and the enzyme requires no cofactors. In addition, hollow fiber reactors appear to offer definite economic advantages due to the extreme ease of reactor construction, enzyme loading, and enzyme regeneration. Also, use of the model presented earlier offers a priori knowledge of enzyme and fiber area requirements for process scale-up to any operating size.

In this section are described experiments performed with commercially available lactase immobilized in asymmetric hollow fibers for lactose hydrolysis in buffered aqueous lactose solutions ("artificial" whey).

#### Materials

Asymmetric hollow fiber tube bundles (type XMH membrane) were generously supplied by Romicon, Inc., Woburn, MA. The hollow fibers were 510 $\mu$ m i.d. and 860 $\mu$ m o.d.; each bundle consisted of 1200 fibers of 50 cm active length potted with epoxy into a 4.5 cm diameter lucite sheath. These bundles were manufactured for industrial ultrafiltration and dialysis, and hence contain larger fibers and more surface area than those used for the  $\beta$ -galactosidase experiments.

Lactase LP, isolated from Aspergillus niger was provided by the Wallerstein Co., Deerfield, IL. Maxilact, isolated from Saccharomyces lactis, was provided by the Enzyme Development Corporation, New York, N.Y. Lactase LP is an acid enzyme with pH activity optimum between 3.5 and 5.5, and as such would find direct use in the treatment of acid whey. In contrast, Maxilact is a neutral enzyme, most active at pH about 7.0, hence it would be more directly applicable to the treatment of sweet whey (for example from cheddar cheese manufacture), neutralized acid whey, or in the production of lactose-free milk. However, early experiments showed that the half life of Maxilact activity was, at most, a few days at 30°C; thus it would be totally unsuitable in an immobilized enzyme reactor. Consequently, the experiments described in this chapter focus on Lactase LP immobilization, since Wierzbicki et al.<sup>17</sup> have reported the activity half-life for Lactase LP to be in excess of 6 months at 55°C.

Acid whey concentrate was provided by Foremost Dairies, Dublin, CA. All other chemicals used were reagent grade. All solutions were prepared in 0.05 M sodium citrate buffer, pH 4.40 $\pm$ 0.05 unless otherwise stated.

The Lactase LP preparation was assayed for protein using both the Biuret reaction (Total Protein Kit No. 540, Sigma Chemical Co., St. Louis, MO) and ultraviolet absorption at 280 nm.; for metal cations using atomic absorption; for glucose using the glucose oxidase/peroxidase reaction with a redox dye indicator (Glucose Reagent Kit No. 510, Sigma Chemical Co.); for galactose using the galactose oxidase/peroxidase reaction with a redox dye indicator (Galactostat Reagent Kit, Worthington Biochemical Corp., Freehold, NJ); for fructose by the method of Messineo and Mussara,<sup>22</sup> and for total hexose using the sulfuric acid-cysteine HCl method.<sup>23</sup> Results showed the preparation to contain, by weight, about 7% protein (presumably predominantly lactase), 3% metal salts, 22% glucose, 32% fructose, and 7% other hexose, though no galactose was found.

#### Enzyme Kinetic Constants

Lactase LP, diluted to approximately 1 mg commercial preparation per ml, was assayed at 35°C in lactose solutions of increasing concentration, ranging from 20 to 100 mM. At zero time, 0.5 ml of enzyme solution was added to a 4.5 ml volume of lactose solution. Between 3 and 15 minutes following mixing the reaction was stopped by adding 0.5 ml of 1.0 M KOH to raise the pH to 12. The amount of glucose produced was measured to determine percent hydrolysis of the initial lactose, thereby permitting computation of the initial reaction rate. Glucose measurements were performed using the glucose oxidase/peroxidase reaction. Since glucose oxidase also catalyzes to a slight extent oxidation of lactose and galactose, care was taken to account for the presence of these two constituents. In addition, corrections were made for the glucose present in the Lactase LP preparation. Since the extent of lactose hydrolysis never exceeded 3% in determinations of the enzyme kinetics, measurements of  $\Delta c/\Delta t$  were indeed representative of initial reaction rates. Linear least squares analysis with unit weights on Lineweaver-Burke double reciprocal plots provided the kinetic constants  $V_{max}$  and  $K_m$ .

The galactose inhibition constant,  $K_i$ , was determined by assaying Lactase LP, in the presence of galactose, using *o*-nitro-phenyl- $\beta$ -d-galactopyranoside (ONPG) as substrate. In two separate determinations galactose concentration was varied over two ranges, from zero to 100 mM and from zero to 10 mM.  $K_i$  was also ascertained using lactose as the substrate with galactose concentration ranging from zero to 10 mM.

#### Substrate Solution

In all reactor experiments the substrate feed solution was "artificial" whey, 5% lactose in citrate buffer, pH 4.4. Enzyme activity determinations using reconstituted acid whey concentrate indicated that no component of acid whey interfered to any measurable extent with Lactase LP activity, as compared to buffered lactose solutions. Therefore the use of "artificial" whey was justified.

The density of the 5% lactose solution over the temperature range 30° to 40°C was measured using a pycnometer. The kinematic viscosity of the solution was measured over the same temperature range using an Ubbelohde viscometer (Cannon Instruments, State College, PA).

#### Reactor Experiments

Two identical fiber bundles, denoted A and B, were used in this study. A reactor was charged with enzyme by pipetting 300 ml of Lactase LP solution into the shell side of the bundle. After overnight storage at 3°C, excess enzyme solution (about 150 ml) was drained and the unit installed. The apparatus was essentially as shown in Figure 3. The enzyme solution drained from the unit was diluted to approximately 1 mg/ml concentration then assayed as described previously to determine  $V_{max}$  and  $K_m$ . Before the start of an experiment approximately 2 liters of buffer was passed through the reactor. Substrate flow was then begun and reactor outlet samples collected at 15 minute intervals until steady state was

reached. Reactor inlet and outlet temperatures were monitored with thermistor probes and were found to differ by no more than 0.8°C over a reactor run. Inlet and outlet pressures were monitored with water manometers. Substrate feed solution was 5% (139 mM) lactose in citrate buffer. The reactor flow rate was measured directly by collecting a volume of outlet fluid in a measured time period.

### Results

#### 1. Determination of $K_i$

Lineweaver-Burke plots of the data obtained for the determination of  $K_i$  using ONPG as substrate are shown in Figure 6 for galactose concentrations ranging from (a) zero to 100 mM and (b) zero to 10 mM. Figure 7 shows the slopes of the Lineweaver-Burke plots versus galactose concentration for each determination. Using Figures 6 and 7,  $K_i$  was found to be  $1.9 \pm 0.1$  mM. The value determined using lactose as substrate was virtually identical.

#### 2. Reactor experiments

The data obtained for five reactor runs for various enzyme loadings are shown in Table I.  $V_{max}/K_m$  was measured as described above, using enzyme solution drained from the reactor bundle immediately before use. Other parameters are:  $Q$ , the outlet flow rate,  $\Delta P$ , the difference between inlet and outlet header pressure, and  $T$ , the average of inlet and outlet temperature.

It was observed in early experiments that the number of fibers actually utilized for reaction in the bundle was somewhat less than the 1200 available. Because of the reactor installation procedure and the use of non-degassed feed, a significant number of air bubbles were introduced into the fibers of the bundle and, owing to the very small pressure drops required to cause flow through the bundle, remained trapped within the fibers. Accordingly, a number of fibers were blocked and thus unavailable for reaction.

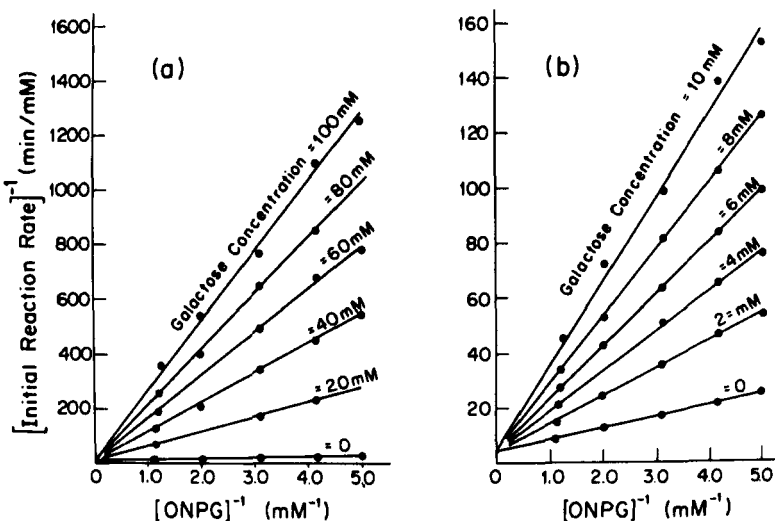


FIGURE 6

Lineweaver-Burke plots used in determining  $K_i$  for Lactase LP. Substrate and inhibitor are ONPG and galactose, respectively. Galactose concentration varies from zero to a) 100mM and b) 10mM.

If Poiseuille flow in each individual fiber is assumed, then the number of fibers through which fluid is flowing may be calculated from

$$N = \frac{8\pi LQ}{4 \Delta P \pi a^4} \quad (3)$$

The measured viscosities of a 5% lactose in citrate buffer solution at reactor temperatures appear in Table I. The number of active fibers,  $N$  in Table I, was calculated from Equation (3) knowing reactor flow rate,  $Q$ , pressure drop,  $\Delta P$ , bundle length  $L = 50$  cm, and fiber radius,  $a = 255\mu\text{m}$ . As shown in Table I,  $N$  for early runs was indeed significantly less than 1200. However, it is possible to clear blocked fibers by increasing the flow rate through (and thus the axial pressure drop across) the bundle, thereby removing

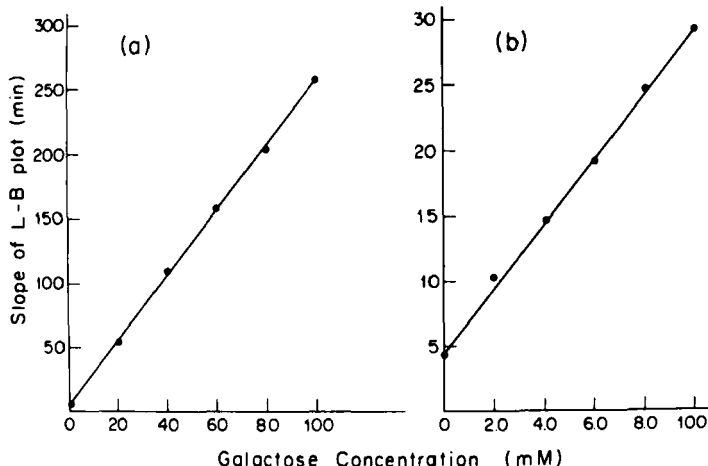


FIGURE 7

Slopes of Lineweaver-Burke plots in FIGURE 6 vs. galactose concentration. Galactose concentration varies from zero to a) 100 mM and b) 10 mM.

entrained air bubbles. This fact is reflected in the increased  $N$  for A3 and A4, where a  $\Delta P$  equivalent to 5 ft  $H_2O$  was applied to the bundle prior to initiating substrate flow.

### 3. Model correlations

With  $K_i$  being 1.9 mM, and expected reactor galactose concentrations in the 100 mM range, the effects of galactose inhibition for this enzyme reactor cannot be neglected as they were for the E. Coli  $\beta$ -galactosidase experiments described earlier. Consequently, the reaction rate within a fiber's porous annulus will be described by the Michaelis-Menten equation with competitive inhibition by one product. This has the effect of adding an additional dimensionless parameter, an inverse inhibition constant,  $\xi = C_o/K_i$ . As such, reactor conversion now depends on eight dimensionless parameters.

TABLE I  
Lactase Reactor Data

Run	$\frac{V_{max}}{K_m} \times 10^2$ (sec <sup>-1</sup> )	Q (ml/min)	ΔP (in. H <sub>2</sub> O)	T (°C)	μ (cp)	N
A1	1.04±.08	20.7	1.78	34.1	0.863	205
		8.70	0.82	33.1	0.881	191
		3.28	0.44	31.7	0.903	137
A2	2.08±.24	21.1	1.37	34.3	0.859	270
		9.56	0.63	33.7	0.870	269
		3.30	0.26	31.8	0.904	234
B1	0.39±.06	21.1	1.30	34.1	0.863	286
		9.12	0.60	32.4	0.893	277
		3.05	0.22	30.1	0.935	264
A3	2.09±.17	21.8	0.71	34.9	0.848	531
		9.09	0.30	34.6	0.854	528
		3.45	0.12	33.3	0.877	514
A4	1.03±.03	20.8	0.51	34.6	0.853	710
		9.37	0.24	34.7	0.852	679
		3.57	0.11	33.6	0.872	577

For the five reactor runs shown in Table I,  $K_m$  was determined to be  $26.8 \pm 10.5$  mM, and  $K_i$  was previously measured to be  $1.9 \pm 0.1$  mM. Therefore, for these experiments, with a feed solution concentration of 139 mM

$$\frac{b}{a} = 1.0008$$

$$\frac{d}{a} = 1.7$$

$$\frac{d_1}{d_3} = 1.0$$

$$\frac{d_1}{d_2} = 10.0$$

$$\theta = 0.2$$

$$\xi = 70$$

and reactor conversion becomes a function of the remaining two parameters  $\lambda^2$  and  $z$ .

Table II tabulates the reactor data with  $\lambda^2$  and  $z$  calculated using the solution diffusivity of 5% lactose at 35°C,  $5.6 \times 10^{-6}$  cm<sup>2</sup>/sec, 24,25 and the number of active fibers,  $N$ , from Table I. The conversion data in Table II are shown plotted as  $C_B$  versus  $z$  with  $\lambda^2$  as a parameter in Figure 8. The solid lines represent model predictions. Excellent agreement between theory and experiment is evident.

#### Discussion

The experiments described herein were performed to assess the utility and functionality of enzyme immobilization within

TABLE II  
Lactase Reactor Model Parameters

Run	$\lambda^2$	$z$	$1 - C_B$
A1	$1.19 \pm .09$	$0.261 \pm .011$	$0.059 \pm .004$
		$0.578 \pm .030$	$0.141 \pm .009$
		$1.10 \pm .09$	$0.189 \pm .006$
A2	$2.39 \pm .28$	$0.337 \pm .016$	$0.154 \pm .010$
		$0.743 \pm .045$	$0.271 \pm .005$
		$1.87 \pm .16$	$0.437 \pm .022$
B1	$0.449 \pm .067$	$0.357 \pm .019$	$0.041 \pm .004$
		$0.800 \pm .073$	$0.086 \pm .005$
		$2.29 \pm .22$	$0.181 \pm .007$
A3	$2.40 \pm .20$	$0.642 \pm .030$	$0.234 \pm .007$
		$1.53 \pm .12$	$0.401 \pm .038$
		$3.93 \pm .67$	$0.611 \pm .202$
A4	$1.18 \pm .04$	$0.900 \pm .049$	$0.177 \pm .005$
		$1.91 \pm .17$	$0.314 \pm .014$
		$4.26 \pm .42$	$0.429 \pm .013$

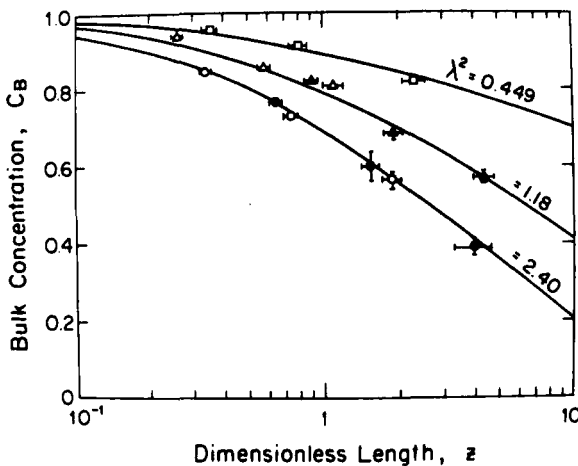


FIGURE 8

Comparison between experimental and predicted reactor conversion as a function of dimensionless reactor length. Solid lines are reactor model predictions.  $\Delta$  Run A1,  $\lambda^2 = 1.18$ ;  $\circ$  Run A2,  $\lambda^2 = 2.39$ ;  $\bullet$  Run A3,  $\lambda^2 = 2.40$ ;  $\blacktriangle$  Run A4,  $\lambda^2 = 1.18$ ;  $\blacksquare$  Run B1,  $\lambda^2 = 0.449$ .

asymmetric hollow fibers as a means of conducting an industrially important conversion, and in this light were quite successful. Although the highest lactose conversion attained in this study was 60%, while industrially interesting conversions would be greater than 80%, the good agreement between experimental data and model predictions implies freedom to choose a priori a sponge-layer enzyme concentration and reactor feed flow rate combination, and attain any desired conversion.

Solubility experiments indicate that Lactase LP is soluble in aqueous solution to about 1 g solids (70 mg protein) per ml solution. At this concentration, Thiele moduli of approximately 200 are possible, and reactor operation in a diffusion limited regime is approached. Although the lactose reactor experiments

were largely kinetically controlled, a two-orders-of-magnitude increase in  $\lambda^2$  to about 100 to 200 would allow approach to conditions of diffusion control, thereby resulting in the most rapid conversion of substrate with reactor length, and a reactor less sensitive to decay of enzyme activity.

The axial enzyme transport phenomenon discussed previously was of no concern in these experiments since the highest bundle pressure drop encountered in the Lactase LP experiments was a factor of eight lower than the highest pressure drop encountered in the  $\beta$ -galactosidase experiments.

#### CONCLUSIONS

The results of this investigation confirm the validity of the asymmetric membrane hollow-fiber-bundle concept as a means for effective enzyme-immobilization, and efficient conversion of membrane-permeable substrates into membrane-permeable products. Of particularly great practical importance is the versatility and adaptability of this reactor concept to a wide variety of enzymes and enzymatic reactor systems, and to both industrial- and laboratory-scale conversions. Of noteworthy theoretical interest is the ease and accuracy with which this system can be modelled by classical chemical kinetic-, diffusion-, and fluid mechanical theory, and its dynamic performance thereby predicted and correlated.

While the membrane-hollow-fiber system has so far been tested only with immobilized enzymes, the reactor concept is clearly of interest and potential utility for any catalytic reaction wherein the catalyst can be impounded within the fiber-wall, and where reactants and products have free access (by convection or diffusion) to and from the catalytic sites or surfaces. Further research to establish the generic suitability of hollow semipermeable membrane fiber systems as continuous flow catalytic reactors is contemplated.

NOMENCLATURE

a	inner radius of fiber (cm)
b	(b-a) is the thickness of the membrane region of the wall (cm)
C	substrate concentration
d	(d-b) is the thickness of the sponge region of the fiber wall (cm)
D	substrate diffusivity (cm <sup>2</sup> /s)
K <sub>m</sub>	Michaelis constant (mole/cm <sup>3</sup> )
K <sub>i</sub>	product inhibition constant (mole/cm <sup>3</sup> )
L	reactor length (cm)
N	number of fibers
ΔP	pressure difference (in. H <sub>2</sub> O)
Q	substrate flow rate (cm <sup>3</sup> /s)
T	temperature (°C)
v <sub>0</sub>	maximum velocity (cm/s)
v <sub>max</sub>	maximum reaction rate (mole/cm <sup>3</sup> ·s)
x	dimensionless axial coordinate, normalized with respect to L
z	$\zeta/\alpha$ dimensionless axial coordinate

Greek Letters

α	$v_0 a / \frac{D}{L}$ Péclet number
γ	membrane partition coefficient
θ	$K_m / C_o$
λ <sup>2</sup>	$V_{max} a^2 / K_m D$ Thiele modulus
μ	viscosity (poise)
ξ	$C_o / K_i$
ζ	axial distance (cm)

Subscripts

0	inlet
1,2,3,4	region
B	bulk

ACKNOWLEDGEMENTS

The authors acknowledge with thanks the support of the Petroleum Research Fund, administered by the American Chemical Society (PRF 7295 AC4, 7); and the Engineering Foundation, United Engineering Trustees, Inc. (RC-A-73-5), in the conduct of this research, and the National Science Foundation for support in the form of a Traineeship held by L. R. Waterland. The assistance given us by the Amicon Corporation, Lexington, Massachusetts, and by Mr. Michael Lysaght of that company is gratefully appreciated.

REFERENCES

1. R. Goldman, L. Goldstein and E. Katchalski, in "Biomedical Aspects of Reactions at Solid Surfaces," G. R. Stark, ed., Academic Press, N. Y., 1971, p. 1.
2. H. D. Brown and F. X. Hasselberger, in "Chemistry of the Cell Interface," Part B, H. D. Brown, ed., Academic Press, N. Y., 1971, p. 185.
3. R. G. Carbonell and M. D. Kostin, *AIChE J.*, 18, 1 (1972).
4. I. H. Silman and E. Katchalski, *Ann. Rev. Biochem.*, 35, 873 (1966).
5. O. R. Zaborsky, "Immobilized Enzymes," CRC Press, Cleveland, 1973.
6. T. M. S. Chang, F. C. McIntosh and S. G. Mason, *Can. J. Physiol. Pharm.*, 44, 115 (1966).
7. P. R. Rony, *Biotech. Bioeng.*, 13, 431 (1971).
8. P. R. Rony, *JACS*, 94, 8247 (1972).
9. R. A. Cross, *AIChE Symp. Ser.*, 68(120), 15 (1972).
10. L. R. Waterland, A. S. Michaels and C. R. Robertson, *AIChE J.*, 20, 50 (1974).
11. K. Wallenfels and R. Weil in "The Enzymes," Vol. VII, 3rd Ed., P. D. Boyer, ed., Academic Press, New York, 1972.
12. K. Wallenfels and O. P. Malhotra, in "The Enzymes," Vol. IV, 2nd Ed., P. D. Boyer, H. Lardy and K. Myrbaech, eds., Academic Press, New York, 1972.

13. L. R. Waterland, C. R. Robertson and A. S. Michaels, *Chem. Eng. Commun.*, 2, 37 (1975).
14. M. D. Lilly, K. Balasingham, D. Warburton and P. Dunnill, in "Fermentation Technology Today," Proc. IV Fermentation Symposium, G. Terui, ed., Society for Fermentation Technology, Japan, 1972, p. 379.
15. I. Chibata, T. Tosa, T. Salo, T. Mori and Y. Matsuo, in "Fermentation Technology Today," Proc. IV Fermentation Symposium, G. Terui, ed., Society for Fermentation Technology, Japan, 1972, p. 383.
16. B. H. Webb and E. O. Whittier, "Byproducts from Milk," Avi, N. Y., 1970.
17. L. E. Wierzbicki, V. H. Edwards and F. V. Kosikowski, *Biotech. Bioeng.*, 16, 397 (1974).
18. H. H. Weetall, N. B. Havewala, W. H. Pitcher, Jr., C.C. Detar, W. P. Vann and S. Yaverbaum, *Biotech. Bioeng.*, 16, 295 (1974).
19. H. H. Weetall, N. B. Havewala, W. H. Pitcher, Jr., C. C. Detar, W. P. Vann and S. Yaverbaum, *Biotech. Bioeng.*, 16, 689 (1974).
20. F. X. Hasselberger, B. Allen, E. K. Paruchuri, M. Charles and R. W. Coughlin, *Biophys. Biochem. Res. Comm.*, 57, 1054 (1974).
21. A. C. Olson and W. L. Stanley, *J. Agr. Food Chem.*, 21, 440 (1973).
22. L. Messineo and E. Musarra, *Int. J. Biochem.*, 3, 691 (1972).
23. G. Ashwell, in "Methods in Enzymology," Vol. III, S. P. Colowick and N. O. Kaplan, eds., Academic Press, N. Y., 1957.
24. L. G. Longsworth, in "American Institute of Physics Handbook," D. E. Gray, ed., McGraw-Hill, N.Y., 1957.
25. "International Critical Tables of Numerical Data, Physics, Chemistry, and Technology," Vol. V, E. W. Washburn, ed., McGraw-Hill, N.Y., 1929.